Suplemento de la Revista Mexicana de Física **1** (1) 13-17 JANUARY-MAY 2020

Evolution of rectangular and triangular initial beam profiles in positive Kerr local medium

M. Hesami[a], M. Avazpour[b], M. M. Méndez Otero[b], and J. Jesús Arriaga Rodriguez[a]
[a]*Instituto de Física, "Ing. Luis Rivera Terrazas", Benemérita Universidad Autónoma de Puebla, Av. San Claudia Y BLVD. 18 sur, Col. San Manuel, C.P. 72570, Puebla, Puebla, México.*
e-mail: maj.hesami@gmail.com
[b]*Facultad de Ciencias Físico Matemáticas, Benemérita Universidad Autónoma de Puebla, Av. San Claudio y 18 Sur. Col San Manuel, C.P. 72570, Puebla, Puebla, México.*

Received 14 August 2019; accepted 11 September 2019

The hyperbolic secant (Sech) shape, as the initial beam profile, is the well-know profile that compensates the diffraction and self-focusing effect during propagation in Kerr medium, and evolves as the bright spatial soliton. The Sech beam can be confined in the Kerr medium and induces its own waveguide. In this work, two initial beam profiles, rectangular and triangular functions, that are different than Sech profile, are considered, and the propagation of these beam profiles in third-order nonlinear (Kerr) medium is investigated. As a result, the initial beam-width played an important role in confining the beam profiles in direction of propagation. In addition, the intensity profiles change to the Sech profile after some initial step of propagation. All the calculations and simulations have been done by the Split-Step numerical method with MATLAB program.

Keywords: Spatial soliton; positive Kerr medium; local medium; nonlinear Schrödinger equation.

PACS: 42.65. Jx

DOI: https://doi.org/10.31349/SuplRevMexFis.1.13

1. Introduction

The term soliton derived from solitary wave. Although the solitary waves generate their own channel, remain localized and conserving their shape as they travel, they can be significantly changed by colliding with one another. However, solitons are solitary waves that do not change their shape by collision [1-3]. The soliton was first observed by Scott Russell [4]. The study and observation of solitons are not limited just for the optical area and it is included in many fields from fluids to solid-state and chemical systems [5-7]. The interest in optical solitons is growing due to their application for fast transferring data through the beam-light, for example, by compressing the temporal pulse duration in long-distance communication via fiber optics [8,9]. However, in other applications, the broadening of pulse duration or compressing the spectral is done by researchers [10]. Bounded self-guided beams in space, or more precisely spatial solitons, evolve from a nonlinear change in the refractive index of a material, induced by the distribution of light intensity. For the special case where, the exact compensation occurs between the refractive nonlinearity and the beam diffraction, the beam profile can be self-trapped and propagates without change in its shape. Likewise, the same phenomenon is through for temporal solitons or localized pulses in time. Due to the light-induced refractive index, once the compensation between the refractive nonlinearity and the pulse dispersion is obtained, the pulse propagates without change in shape, and the pulse is self-trapped [11]. Obtaining the optical solitons requires an intense beam or laser light in the appropriate profile as solution of the Nonlinear Schrodinger (NLS) equation. Spatial solitons are kinds of beam that create their own induced waveguide Kerr medium due to intensity dependent of induced refractive index [12,3,13]. In this case, the main nonlinear equation in the form of cubic Nonlinear Schrodinger (NLS) equation governs the beam evolution. For the complex amplitude of the electric field, the NLS equation has two distinct types of localized solutions, bright and dark solitons, depending on the sign of the group-velocity dispersion (for temporal soliton) or Kerr coefficient (for spatial soliton). The NLS equation for the positive Kerr medium, Eq. (1), allows a fundamental bright soliton solution, holding the profile of hyperbolic secant (Sech) with appropriate amplitude and width [14,15], however in negative Kerr medium, the NLS equation permits the hyperbolic tangent beam profile as fundamental dark soliton solution [16].

In this work, in positive Kerr medium the evolution of rectangular and triangular beam profiles as the initial conditions are used, where these initial profiles are different from Sech. Also, the effect of the initial beam-width over the evolution of intensity profile is investigated. Although the two considered profiles are not the analytical solution of the NLS equation in positive Kerr medium, numerically we are simulating and demonstrating that by considering the adequate initial width, it is possible to propagate the beam in the direction of propagation while spatially the intensity profile is confined. By increasing the initial beam-width bigger than the adequate one, the intensity profile suffers higher oscillation by propagation along the direction of propagation, however by decreasing the initial-width, the intensity profile decays and is affected by diffraction effect, rather than nonlinear (self-focusing) effect. Finally, it is showed that the intensity profile of the considered initial conditions evolve to a specific Sech profile. To validate this reality, we have com-

pared the propagated profile at different propagation distance Z with our proposed Sech function (Sech-Test). The Split-Step method [14] is used for numerical study in MATLAB program.

2. Numerical experiment

In the nonlinear medium with third-order of nonlinearity (Kerr medium), $\Delta n = n_2 I$ is the induced change of refractive index, where n_2 is the Kerr coefficient. The induced refractive index has a dependency on the intensity of beam $n = n_0 + n_2 I$, where n_0 is the linear refractive index. The Paraxial evolution of (1+1)-dimensional beam, with field amplitude of $E = E(x,z)\exp(ikZ)$ in Kerr medium is governed by the NLS as follows in Eq. (1).

$$-i\frac{\partial A(X,Z)}{\partial Z} = \frac{1}{4}\frac{\partial^2 A(X,Z)}{\partial X^2} \pm \frac{L_D}{L_{NL}}|A(X,Z)|^2 A(X,Z), \qquad (1)$$

where $A(X,Z)$ is the amplitude of the beam field normalized to $(\sqrt{I_m})$, the maximum initial intensity. $L_D = n_0 k_0 x_0^2/2$ is the diffraction length or the Rayleigh distance, x_0 is a transverse scaling parameter related to the input beam-width, and $X = x/x_0$ and $Z = z/L_D$ are the transversal and longitudinal distance normalized to the initial beam-width, and the Rayleigh distance respectively. $L_{NL} = 1/n_2 k_0 I_m$ is the self-focusing distance, $k_0 = 2\pi$ the wavenumber, λ the wavelength. Positive and negative signs correspond to the positive and negative materials that have a direct relation to the sign of the Kerr coefficient, n_2. The maximum initial intensity, I_m, has to be in the specific value in order the ratio between L_D and L_{NL} becomes one ($L_D/L_{NL} = 1$), otherwise when other relation is valid such as ($L_D/L_{NL} = N$), there is the possibility of the evolution as the higher-order solitons [17]. For the positive materials ($n_2 > 0$), and the relation of $L_D/L_{NL} = 1$, the NLS equation, Eq. (1), allows the analytical and fundamental solution of bright soliton in the form of the Sech beam profile (see Eq.(2)), where the beam propagates as the solitary beam profile, and conserves its occupied transversal space during the propagation. To obtain the perfect bright spatial soliton by Sech as the initial profile, the width of $b_s = 0.7071$ mush be considered. When smaller values of b_s are chosen, the intensity profile propagates as the diffracted beam, while for wider beam-width high oscillatory behavior is detected by propagation. The critical initial power of the Sech is $P_s = 1.4142$

$$\left(P_s = \int_{-\infty}^{+\infty} |A_s(X)|^2 dX = 1.4142\right).$$

$$A_s(X) = 1 * \sec h\left(\frac{X}{b_s}\right) = 1 * \sec h\left(\frac{X}{0.7071}\right). \qquad (2)$$

Since it is considered that the medium is not losing energy and there is not any amplification on energy (for example, Erbium doped fibers can amplify the intensity of a beam in fiber optics [18]), the Sech initial beam profile propagates as spatial soliton and is continued forever. Here the evolution of two profiles different from the Sech, rectangular Eq. (3) and triangular Eq. (4), as the initial beam profiles are simulated numerically by MATLAB program using the Split-Step method. This method is reliable and commonly used to solve the NLS equation in optical media [19,20]. We are monitoring the effect of considering different initial beam-widths over the evolution of the beam profile. In Eq. (3) and Eq. (4), the $A_R(X)$ and $A_T(X)$ are the amplitude profiles, b_R and b_T are the initial beam-width for rectangular and triangular initial beam profiles respectively.

$$A_R(X) = 1 * Rectpuls\left(\frac{X}{b_R}\right) \qquad (3)$$

$$A_T(X) = 1 * Triangularpulse\left(\frac{X}{b_T}\right). \qquad (4)$$

In Fig. 1, we plot the evolution of these two initial beam distributions along 100 Z, together with its initial and final intensity profile in linear and logarithmic scale. In this figure, the numerical simulation has been done by employing the best initial widths mentioned in Table I. Figure 1 (left column) corresponds to the propagation of the rectangular initial beam profile with $b_T = 2.22$, and (right column) relates to the propagation of the triangular as initial beam profiles with $b_R = 2.30$. Figure 1 row (a) shows the beam intensity propagation in two dimensions, while the beam is launched in medium from the downside. The X is the transversal axis and Z is the longitudinal axis or direction of propagation. The color shows the value of intensity referred on the color bar. A three-dimensional view of propagation appears in Fig.1 row (b), and the normalized intensity profile is plotted in the perpendicular axis. In Fig. 2, the on-axis intensity for triangular (black solid line), and rectangular (red dashed line) are plotted when the best initial beam-widths are considered. The on-axis intensity graph corresponds to the evolution of perfect bright soliton, the Sech (green dot), is plotted in Fig. 2 for making the comparison with the other two line graphs. Some criteria have been used to obtain the best initial beam-widths for both beam profiles in order to confine the intensity profile in the direction of propagation as much as possible, and this can be understood with the help of Fig. 2. In this figure, the on-axis normalized intensity is plotted for both profiles. We have recorded the maximum, $I_{\max}$, and minimum, $I_{\min}$, values of on-axis intensity along 100 Z, also the difference between them, ΔI, $\Delta I = I_{\max} - I_{\min}$ for variety value of initial beam-width. By considering different initial beam-widths, different intensity oscillation ΔI, are recorded. The manner to find the best initial width for both types of beam profiles are in the following: Since for some initial step of propagation, too much oscillation occurs, we did not consider the first 10 Z distance of propagation for obtaining the maximum, $I_{\max}$, and minimum, $I_{\min}$, values of on-axis intensity, but for the rest of direction until 100 Z they are measured, as well as the difference between them, $\Delta I = I_{\max} - I_{\min}$.

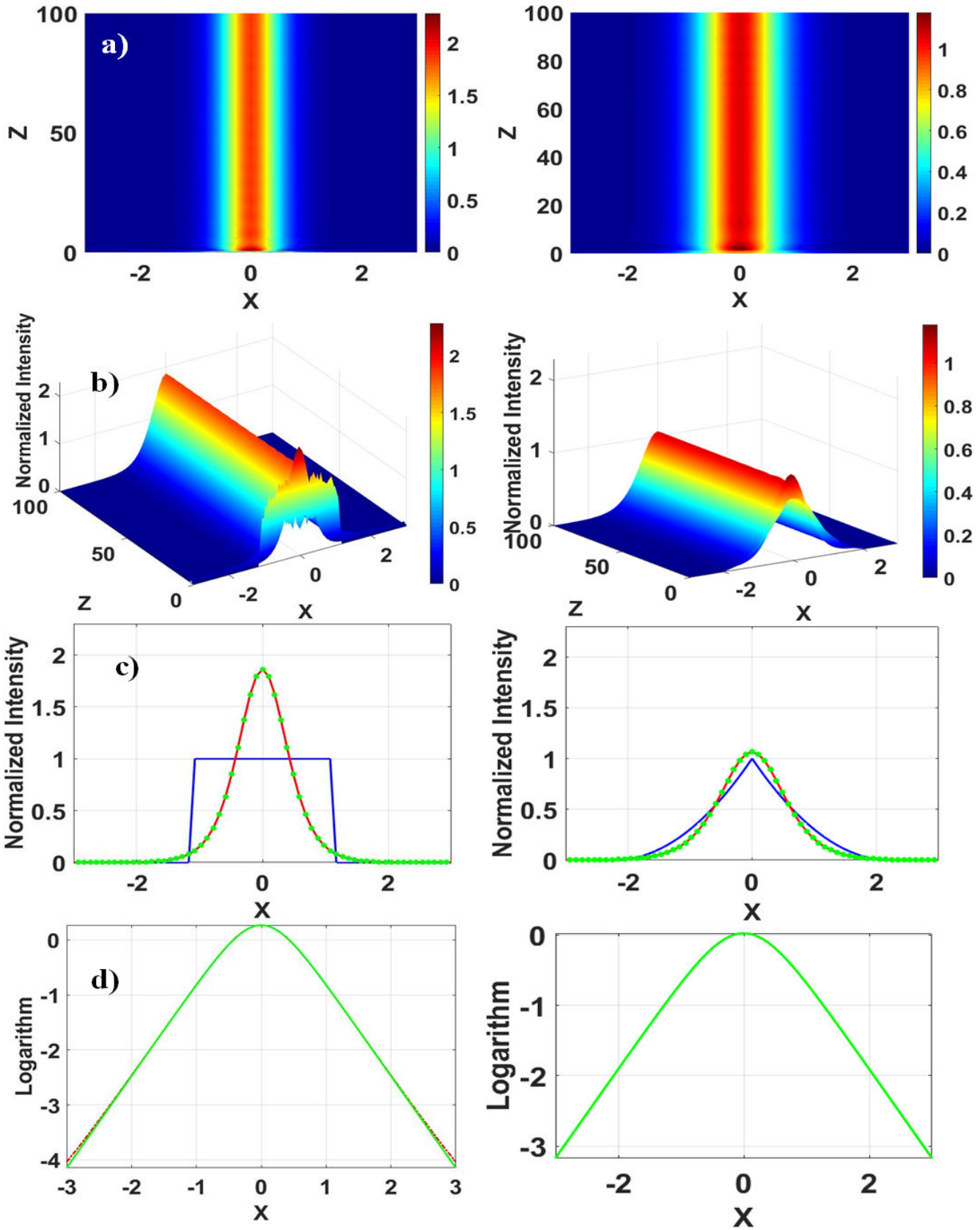

FIGURE 1. Beam intensity Propagation for (a) two and (b) three -dimensional view for 100 Z for: (left side) Rectangular, (right side) Triangular initial field distributions. Intensity profiles in linear (c) and logarithmic (d) scale for: initial (blue-solid line) and final (red-dash dot line) distributions. Sech-Test (Green marks).

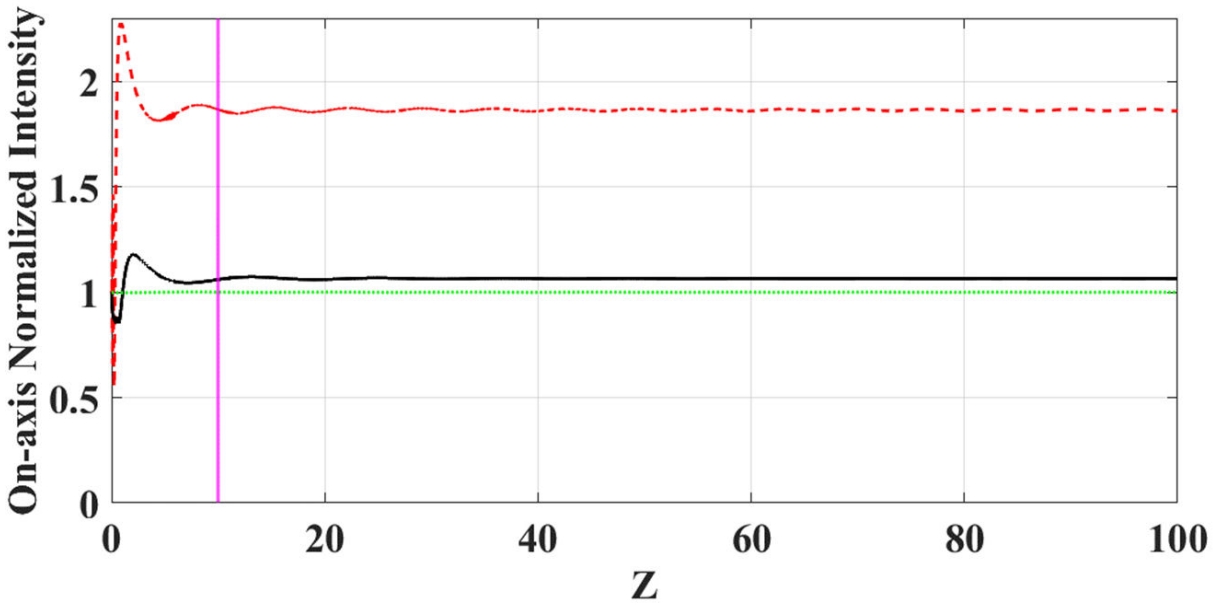

FIGURE 2. On-axis intensity along 100 Z for the following initial fields: Triangular (black, solid line), Rectangular (red, dash line), and Sech as perfect soliton (green dot) with the best initial beam-width mentioned in Table I. As reference, vertical line (pink solid line) at 10 Z.

TABLE I. Best initial beam-width for triangular, rectangular, and Sech profiles.

b	$I_{\max}$	$I_{\min}$	AV_I	ΔI	P_i
$b_T = 2.22$	1.0728	1.0598	1.0663	0.0130	1.4814
$b_R = 2.30$	1.8792	1.8439	1.8616	0.0352	2.2461
$b_s = 0.7071$	1.00	1.00	1.00	0.0001	104142

Then, we changed the initial beam-widths (b_T, and b_R) until the lowest oscillation ΔI, for on-axis intensity is obtained, and this specific value is called the best initial beam-width. These values for initial beam-widths are making the best way to confine the beam intensity in the direction of propagation by almost constant intensity profile with some inevitable on-axis intensity oscillation around average intensity value ($AVI = I_{\max} - I_{\min}/2$). In Table I, the following data is dropped when the best initial beam-width for both profiles have been chosen: the maximum and minimum on-axis intensity values and the difference between them, the average on-axis intensity and the initial power. By considering the initial beam-width higher than the mentioned values in Table I, the initial beam power increases higher than the necessary value to confine the beam in direction of propagation. In this case, the nonlinear effect (the third term in the NLS Eq. (1)) becomes more powerful than the linear effect (the second term in the NLS Eq. (1)). So that, due to the self-focusing effect, the beam-width becomes narrower and the intensity oscillation increases. However, by considering lower value for initial beam-width, the beam profile suffers more diffraction (linear effect) rather than the nonlinear effect, and the intensity profile decays while experiences high oscillations. Though, by adjusting the appropriate initial beam-widths, the intensity profile tends to make balance between the linear effect (diffraction) and the nonlinear effect (self-focusing), then self-reshapes its intensity profiles to a stable one. Since the initial beam profiles (rectangular and triangular) are different than the Sech (the analytical solution of the NLS equation), small oscillations over intensity profiles occur inevitably.

Once the appropriate beam-width is chosen, by evolution of both initial beam profiles (rectangular and triangular), the intensity profiles reshape to an specific shape as is displayed in Fig. 1 row (b). So that here we are going to compare the intensity profile during the propagation with a proposed Sech profile (call it Sech-Test) in the form of Eq. (5):

$$A_{\text{sech}} = A_0(Z)\,\text{sech}\left(\frac{X}{b_X}\right). \tag{5}$$

In this equation, the $A_0(Z)$ is considered as the amplitude of the propagated beam at position Z. Since on-axis intensity during propagation at Z is known, $I_0(Z)$, the amplitude of Sech-Test function is $A_0(Z) = \sqrt{I_0(Z)}$. The b_x is the beam-width of the Sech-Test function which its value is unknown and is obtained in the following. P_i is the initial power of the beam. To obtain the beam-width of the proposed Sech, b_x, the P_i is compared with the power of the proposed Sech-Test. Although the initial power for comparison with the propagated beam is used, it doesn't mean that whole the energy of the beam is confined in the final propagated beam profile.

$$\begin{aligned} p_i &= \int_{-\infty}^{+\infty} \left| A_0(Z)\,\text{sech}\left(\frac{X}{b_X}\right)\right|^2 dX \\ &= 2b_X|A_0(Z)|^2 \rightarrow b_X = \frac{P_i}{2|A_0(Z)|^2}. \end{aligned} \tag{6}$$

Once the b_x is obtained, the intensity profile of the beam during the propagation is compared with our proposed intensity function $I_{\sec h}$, Eq. (7).

$$I_{\mathrm{sec}h} = \left|A_0(Z)\right|^2 \mathrm{sec}h^2\left(\frac{2|A_0(Z)|^2}{P_i}X\right), \qquad (7)$$

Figure 1 row (C), compares the initial intensity profile (blue solid line), with the final intensity profile (red dashed line), and the intensity of the Sech-Test (green marks). Where the left and right column are for the initial rectangular and triangular beam profile respectively. There is a very good fit between the propagated intensity profile and the Sech-Test intensity function. For having a better view over the similarity between the Sech-Test and the propagated intensity profile, in Fig. 1 row (d), the logarithm of the two profiles appear. In this figure, the intensity profile in logarithmic for the Sech-test (green solid line) and the propagated profile (red dashed dot) are plotted respectively. Very good coincidence and similarity are observed especially at the center.

3. Conclusion

In this paper, a numerical study concerning the propagation of rectangular and triangular initial beam profiles, different from Sech, in positive third-order nonlinearity (Kerr medium) has been done, where the medium is described by the (1+1)-Dimensional Nonlinear Schrodinger Equation. The Sech profile is the well-known fundamental solution of the NLS equation, which evolves as the spatial bright soliton. At first, we have investigated the evolution of two profiles, rectangular and triangular, in a positive Kerr medium. Then, the effect of initial beam-width has been studied. Since the two considered profiles, rectangular and triangular, are not the analytical solution of the NLS equation, they are not confined in the direction of propagation as they propagate. Therefore, high oscillation or decay of intensity profile by the propagation occurs until the appropriate initial beam-width is chosen. It is demonstrated that, by adjusting the suitable beam-width, the beam can be confined in the direction of propagation with small inevitable oscillation. The results showed that the confined beam is in the form of a Sech profile, and the results compared with our proposed Sech-Test. A good fit between the propagated intensity profile and the Sech-Test intensity profile has been obtained. In other words, when the adequate initial beam-width is considered, after some initial step of propagation, the beam intensity profile reshapes to the form of the Sech profile. When there is not appropriate facility to produce Sech as the initial beam profile to produce the bright solitons, it is possible to use other profiles such as rectangular and triangular profiles and evolve them as bright spatial solitons.

1. P.G. Drazin and R.S. Johnson, *Solitons: an introduction* **vol 2**, (Cambridge university press, 1989).
2. A.W. Snyder and A.P. Sheppard, *Opt. Lett*. **18** (1993) 482-4.
3. A.W. Snyder and D.J. Mitchell, *Science*, **276** (1997) 1538-41.
4. J.S. Russell, *Report on waves 14th meeting of the British Association for the Advancement of Science* **vol 311** (London, 1894), pp 1844.
5. M. Remoissenet, *Waves called solitons: concepts and experiments*, (Springer Science and Business Media, 2013).
6. G.P. Agrawal, *Nonlinear fiber optics* (Accademic Press Optics and Photonics series, San Diego, 2001).
7. A. Hasegawa and Y. Kodama, *Solitons in optical communications* (Oxford University Press, USA, 1995).
8. G.P. Agrawal, *Fiber-optic communication systems* **vol 222**, (John Wiley and Sons, 2012).
9. G.P. Agrawal, *Nonlinear fiber optics Nonlinear Science at the Dawn of the 21st Century*, (Springer, 2000), pp 195-21.
10. M. Avazpour *et al.*, *Opt. Laser Technol.* **120** (2019) 105692.
11. Y.S. Kivshar and B. Luther-Davies, *Phys. Rep*. **298** (1998) 81-197.
12. A.W. Snyder, D.J. Mitchell, L. Poladian and F. Ladouceur, *Opt. Lett*. **16** (1991) 21-3.
13. D.R. Martinez, M.M.M. Otero, M.L.A. Carrasco and M.D.I. Castillo, *J. Phys. Sci. ppl.* **1** (2011) 196.
14. S. López Aguayo, J.P. Ochoa-Ricoux and J.C. Gutiérrez-Vega, *Rev. Mex. Fis. E* **52** (2006) 28-36.
15. J.P. Gordon, *Opt. Lett*. **8** (1983) 596-8.
16. M. Hesami, M. Avazpour, M. Otero and M.D.I. Castillo, *Optik* (2019) 163892
17. M. Hesami, M. Avazpour and M. Otero, *Optik* (2019) 163695.
18. L.A. Rodriguez-Morales *et al*., *OSA Contin*. **1** (2018) 416-25.
19. G. Agrawal, *Applications of nonlinear fiber optics*, (Elsevier, 2001).
20. M. Hesami *et al*., *Optik* (Stuttg). **202** (2019) 163504.